

Emergent coding phases and hardware-tailored quantum codes

Gaurav Gyawali,^{1,*} Henry Shackleton,^{2,3} Zhu-Xi Luo,^{3,4} and Michael J. Lawler^{5,1,3,†}

¹*Department of Physics, Cornell University, Ithaca, NY 14850, USA*

²*Department of Physics, Massachusetts Institute of Technology, Cambridge, MA 02139, USA*

³*Department of Physics, Harvard University, Cambridge, MA 02138, USA*

⁴*School of Physics, Georgia Institute of Technology, Atlanta, Georgia 30332, USA*

⁵*Department of Physics, Applied Physics, and Astronomy,
Binghamton University, Binghamton, NY 13902, USA*

(Dated: March 20, 2025)

Finding good quantum codes for a particular hardware application and determining their error thresholds is central to quantum error correction. The threshold defines the noise level where a quantum code switches between a coding and a no-coding *phase*. Provided sufficiently frequent error correction, the quantum capacity theorem guarantees the existence of an optimal code that provides a maximum communication rate. By viewing a system experiencing repeated error correction as a novel form of matter, this optimal code, in analogy to Jaynes’s maximum entropy principle of quantum statistical mechanics, *defines a phase*. We explore coding phases from this perspective using the Open Random Unitary Model (ORUM), which is a quantum circuit with depolarizing and dephasing channels. Using numerical optimization, we find this model hosts three phases: a maximally mixed phase, a “ \mathbb{Z}_2 code” that breaks its $U(1)$ gauge symmetry down to \mathbb{Z}_2 , and a no-coding phase with first-order transitions between them and a novel *zero capacity multi-critical point* where all three phases meet. For the \mathbb{Z}_2 code, we provide two practical error correction procedures that fall short of the optimal codes and qualitatively alter the phase diagram, splitting the multi-critical point into two second-order coding no-coding phase transitions. Carrying out our approach on current noisy devices could provide a systematic way to construct quantum codes for robust computation and communication.

I. INTRODUCTION

Overcoming decoherence in quantum devices, a fundamental challenge in quantum information science, ultimately requires a system-level optimization approach. A key aspect is tailoring the quantum error correction to the physical platform’s noise and architecture [2–5], i.e., code-level optimization. The central goal here is to find a coding phase—a logical subspace and error correction circuit that, through repeated application, enables, in principle, quantum information to persist for exponentially long times in the number of qubits. Identifying the existence of such a coding phase is a necessary aspect of the design of fault-tolerant quantum computers.

Identifying phases is a common problem in the study of statistical mechanics, which seeks to uncover the equilibrium properties of matter. Jaynes showed that this pursuit is fundamentally an information problem by deriving thermodynamics from the maximum entropy principle [6, 7]. From this angle, phases of matter in quantum systems are identified by determining a density matrix ρ_{eq} that optimizes the von Neumann entropy $S(\rho)$, often subject to known constraints on the problem and rephrased as a minimum free energy principle[8]. The resulting optimum gives rise to different phases, many with emergent properties like magnetism, superconductivity, and topological edge modes. Identifying a coding

phase turns out to be a similar mathematical problem.

The maximum rate of reliable quantum information transmission through a channel, known as the quantum capacity, is determined by a maximum coherent information principle, or minimum relative entropy [9–13]. Associated with this maximum is a density matrix ρ_0 , which determines the initial state, code space, and error correction routines. By analogy with statistical mechanics, solving this optimization problem gives rise to emergent coding phases due to the optimal state needing to satisfy complex many-body entanglement relationships.

We seek fundamental insights into tailoring quantum codes to hardware by studying emergent coding phases of large-scale, noisy quantum channels via optimization of coherent information. To this end, we introduce the open random unitary model (ORUM) consisting of two-qubit depolarizing channels arising from random unitary processes that compete with one-qubit dephasing channels arising from measurements. Numerically analyzing the ORUM’s single-use quantum capacity, we discover a rich phase diagram with two first-order transitions between distinct optimal codes, meeting at a zero-capacity tricritical point. The infinitely continuous nature of the tricritical point highlights the unique interplay of noise and coding in this non-equilibrium setting. While the quantum capacity represents an idealized limit, implementing practical (necessarily suboptimal) decoding schemes alters this phase diagram, demonstrating the sensitivity of coding phases to non-universal or implementation details. Inspired by the structure of optimal codes and the quantum capacity theorem, we find that even these sub-optimal schemes can achieve exponentially long informa-

* Correspondence email address: gg454@cornell.edu

† Correspondence email address: mlawler@binghamton.edu

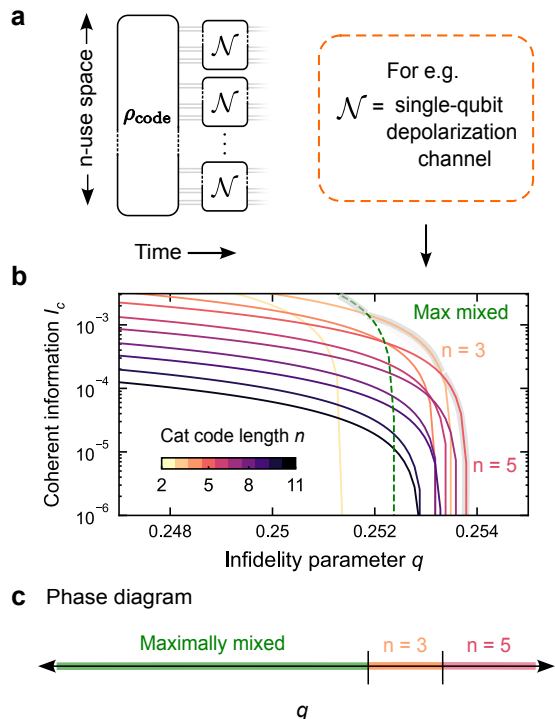


FIG. 1. **Coding transition and superadditivity of the one-qubit depolarizing channel.** **a**, A general depiction of the many-body problem associated with many uses of a quantum channel \mathcal{N} . **b**, A reproduction of the discovery of superadditivity in the coherent information associated with n -uses of the depolarizing channel[1]. While at low noise, the maximally mixed code wins, a 3-qubit cat code yields the highest coherent information I_c at higher q , and a 5-qubit cat code wins at still higher q . No other cat codes competing out to 11-qubit cat codes. **c**, The coding phase diagram associated with discontinuities in the quantum capacity out to 10-uses as the depolarizing error rate q is varied.

tion storage times below certain noise thresholds. Our work reveals a concrete connection between a system’s noise profile and emergent coding phases, suggesting a pathway for hardware-informed code design and targeted noise mitigation strategies by improving the most sensitive noise rates in a coding phase diagram.

Fig. 1b shows a classic example of the discovery of emergent codes and coding phases. Following Ref. 1, we first define a family of n -qubit “cat code” states,

$$\rho_{\text{cat}}^n = \frac{1}{2} (|000\dots\rangle\langle 000\dots| + |111\dots\rangle\langle 111\dots|). \quad (1)$$

We then send each of their qubits through a one-qubit depolarizing channel \mathcal{U}_1 with fidelity q , and compute their coherent information for this process. We call these states codes because the state and its coherent information provide all the information needed to build a quantum code and establish a coding phase, as we will reveal in the paragraphs below. Among the 10 such states presented, the 5 qubit cat code state has the highest coherent information and is therefore the optimal such code

given we are allowed up to 10 uses of the channel. The surprise that such multiple uses of a channel can enable more information to be sent through it per qubit is known as the superadditivity property[14, 15] of the coherent information[13]. It implies that the optimal state for an infinite number of uses, i.e.

$$Q^{(n)} = \max_{\rho} \lim_{n \rightarrow \infty} I_c(\mathcal{U}_1^{\otimes n}, \rho)/n, \quad (2)$$

is a challenging problem and it turns out, in this case, it is still unknown[13, 16–18]. We then identify $Q^{(10)} = Q^{(5)}$ with ρ_{cat}^5 the optimal state of the 10-use quantum capacity in the region $q \lesssim 0.252$, where q is close to the threshold value, but recognize at a smaller value of q , it abruptly goes through a *first order coding phase transition* to $Q^{(10)} = Q^{(3)}$ with ρ_{cat}^3 the optimal state. In this way, though the analog of a thermodynamic limit is now more complex, $Q^{(n)}$ plays a role in coding phases analogous to thermodynamic potential in statistical mechanics.

Let’s turn to a more complex model and explore its phase diagram. Consider the open random unitary model (ORUM), consisting of a brickwork layering of two-qubit depolarizing channels with error rate q_U and one qubit dephasing channels with error rate q_z , schematically depicted by the master equation in Fig. 2a. Depolarizing channels can arise from averaging over unitaries, and dephasing channels can arise by averaging over measurements outcomes. The ORUM has a $U(1)$ gauge symmetry as discussed in supplementary information (SI) Section 1. In the $Q^{(1)}$ of a single time step of Fig. 2a, we identify a large no-coding region with vanishing Q , consistent with the theoretical bound requiring its presence above $q_U = 0.5$ [19]. At lower q_U , we find two distinct coding phases with $Q > 0$, the “ \mathbb{Z}_2 code” and the “maximally-mixed code,” defined below. These initial states were found by direct numerical optimization of the coherent information for one channel use as discussed in SI Section 1. Therefore, by moving to a many-channel problem inspired by quantum circuit models, we obtain a richer set of coding phases than in our first example.

The \mathbb{Z}_2 code is a cat code-like state

$$\rho_{\mathbb{Z}_2} = \frac{1}{2} (|\text{even}\rangle\langle \text{even}| + |\text{odd}\rangle\langle \text{odd}|), \quad (3)$$

where the $|\text{even}\rangle/|\text{odd}\rangle$ state is, up to an arbitrary $U(1)$ gauge transformation, an equal amplitude superposition of all computational basis states with an even/odd number of qubits in their $|1\rangle$ state. The \mathbb{Z}_2 code breaks the $U(1)$ gauge symmetry of the ORUM model down to a global \mathbb{Z}_2 symmetry. We discuss more details of the \mathbb{Z}_2 code in SI Section 2. As the inset shows, it occupies a vanishing region of the phase diagram in the $N \rightarrow \infty$ thermodynamic limit, though superadditivity, as in the cat code example above, could change this conclusion. The maximally mixed code is the maximally mixed initial state, and deriving codes from it is more complex with one approach using absolutely maximally entangled

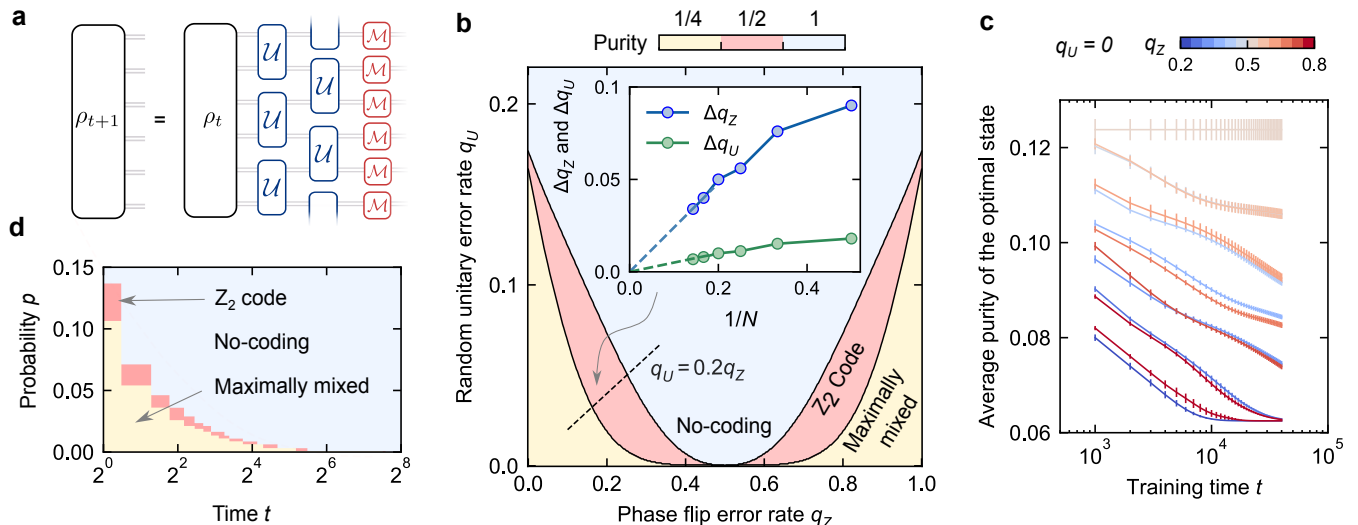


FIG. 2. **Phase diagram of open random unitary model (ORUM)** **a**, A quantum channel-based master equation for ORUM. **b**, Single-use phase diagram of the ORUM for a single time step showing the maximally mixed code, \mathbb{Z}_2 code, and no-coding regions. The inset shows the width of the \mathbb{Z}_2 code decays like $1/N$ with the system size N along the dashed black line given by $q_U = 0.2q_Z$. **c**, Average purity of the optimal state found by the gradient-descent based optimizer showing divergence in optimization time close to the critical point $q_{Zc} = 0.5$. **d**, Dynamical phase diagram of the ORUM obtained by taking $p = 2q_Z/q_U$.

states[20]. The highlight of the whole phase diagram is the zero capacity continuous critical point at $q_U = 0$, $q_Z = 1/2$. The vanishing channel capacity at $q_Z = 0.5$ can be inferred from the Hashing bound [13]. We analytically study the second-order phase transition and show $Q^{(1)}$ is infinitely differentiable along the entire line $q_U = 0$. We further show, in Fig 2c, that the optimization time near this critical point diverges exponentially, demonstrating the existence of a complex set of suboptimal states near this point. Thus, in addition to containing more coding phases, ORUM has a complex coding phase diagram with diverging length scales at a novel *zero-capacity continuous critical point* signified not by a singularity in $Q^{(1)}$ but by it vanishing at just one point.

The one time-step ORUM phase diagram in Fig. 2 represents an ideal limit, an achievable coding phase diagram according to quantum capacity theorem proofs[10–13]. A positive Q value is an achievable communication rate when we send quantum information through one time step and recover it perfectly on the other side. Repeating this t times shows we can, in principle, preserve quantum information for any t . Likely, any other error correction than that used in the quantum capacity proofs will produce subdominant results, and the phase diagram will change. A key aspect of the proof is to build an encoder and an error-correcting decoder out of the initial state, but this construction in the proof is resource-intensive. So the challenge is, can we build a practical, tailored code for a given noise profile that exploits knowledge of the optimal initial state to achieve a high communication rate yet requires low overhead to implement?

Let us approach this problem with the \mathbb{Z}_2 code as a

primary example. It turns out to be a cat code in the X -basis if we set all the arbitrary phases to zero. It is therefore a well known classical $[N, 1, N]$ code, when N is odd, that can correct up to $(N - 1)/2$ simultaneous phase-flip

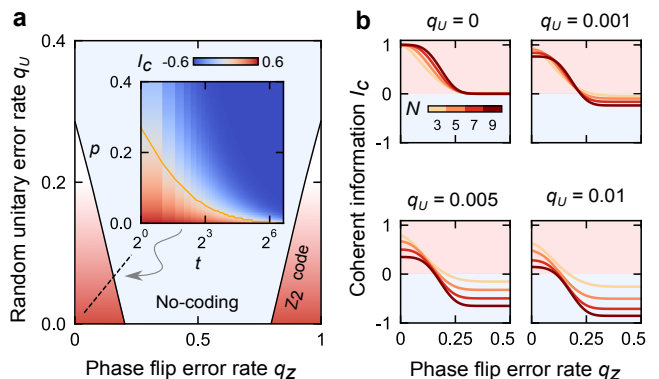


FIG. 3. **Single-use phase diagram with QEC.** **a**, Phase diagram of the \mathbb{Z}_2 code for a 3-qubit random unitary model (ORUM) with periodic quantum error correction (QEC) applied. At long times, the \mathbb{Z}_2 Code vanishes from the $q_U > 0$ region of the phase diagram depicted by the fading red color but survives at $q_U = 0$ for $q_Z \lesssim 0.25$ and $q_Z \gtrsim 0.75$. The inset shows the computed dynamics of coherent information along $p = 2q_Z/q_U$, showing the phase vanishing in constant time along a line cut. **b**, Coherent information of the \mathbb{Z}_2 code, scanning along the q_Z axis with q_U fixed at 0, 0.01, 0.005, and 0.01 respectively for various system sizes N at $t = N$. Finite-size scaling of the $q_U = 0$ (top left) plot suggests a second-order phase transition around $q_Z = 0.25$ (and similarly for $q_Z = 0.75$) not shown.

errors. The error syndromes are known to be the parity checks $X_j X_{j+1}$ for $j \in [0, N-1]$. Correcting phase-flip errors using syndrome extraction and error correction every time step produces a drastic change to the phase diagram, as presented in Fig. 3. Due to the absence of bit-flip errors at $q_U = 0$, the infinitely differentiable zero-capacity critical point splits into coding-no-coding second-order phase transitions at $(q_z, q_U) \approx (0.5 \pm 0.25, 0)$, and the no-coding region grows to fill all $q_U > 0$. The situation is, therefore, analogous to q_U playing the role of temperature with coding phases existing at $q_U = 0$ but not at any finite q_U due to the proliferation of bit-flip errors. Though a qualitative change to the original ideal phase diagram of Fig. 2, this coding phase diagram is realizable in modern quantum devices.

Correcting phase flip errors alone, while progress, is still far from the quantum error correction we need to produce coding phases in general. We can improve our code further by exploiting the multiple channel uses part of Devetak's quantum capacity theorem proof. The simplest way to exploit multiple channel uses is to employ repetition. We replace the $|\text{even}\rangle$ codeword of our $\rho_{\mathbb{Z}_2}$ initial state with, multiple copies of it $|\text{even}\rangle^{\otimes m}$ and similarly for $|\text{odd}\rangle$. Then, a bit-flip error, which sends $|\text{even}\rangle$ to $|\text{odd}\rangle$ and vice versa, can then be detected as it now moves us out of the code space. Now, starting with the \mathbb{Z}_2 repetition code,

$$\rho_{\mathbb{Z}_2^m} = \frac{1}{2} (|\text{even}\rangle \dots |\text{even}\rangle \langle \text{even}| \dots \langle \text{even}| + |\text{odd}\rangle \dots |\text{odd}\rangle \langle \text{odd}| \dots \langle \text{odd}|) \quad (4)$$

where m denotes the level of repetition, we can build an enhanced set of stabilizers. The original stabilizer code for each subsystem gives us stabilizers $X_i X_{i+1}$ that correct phase flip errors. In addition, the repetition introduces the additional stabilizers $Z_I^N Z_{I+1}^N$, with Z_I^N the product of Pauli Z operators on all N qubits of subsystem I . These enable us to correct bit-flip errors. The result is a $[[mN, 1, \min(m, N)]]$ quantum code with the case $N = 3, m = 3$ just Shor's 9-qubit code. Fig. 4 presents numerical results demonstrating this code and evidence for the expected coding phases in the large- m , large- N limit at $q_U > 0$ where this code corrects arbitrary $(\min(m, N) - 1)/2$ errors.

The above results demonstrate that emergent coding phases arise from the noise models of quantum devices with positive coherent information. Optimizing for communication through a single "time step" provides identification of a phase diagram that sets a target for any sub-optimal code to achieve but that likely such a code falls short. We refer to these codes as emergent because they are built out of the information provided by the optimal state, which arises through the solution of a complex optimization problem. The resulting coding phases bear many similarities to phases in quantum statistical mechanics; a potentially fruitful connection could hasten the arrival of fault-tolerant quantum computing.

Our results show many similarities with the measurement-induced phase transitions (MIPT)[21–26]. Here, coding phases emerge out of a complex interplay between unitary dynamics and monitored (post-selected) measurements. The depolarizing channel in ORUM corresponds to the averaging over random unitaries in monitored circuits common in MIPT studies, while the dephasing channel corresponds to the averaging over measurement outcomes. As the single trajectory information is lost during the process of averaging, the coding phase transitions we observe in ORUM are not the same as the MIPTs. In the latter case, below a critical measurement probability, information can persist for a time that scales exponentially with system size – a defining characteristic of a robust coding transition [25, 26] while in the former, we need to introduce periodic error correcting steps to achieve the same thing. Although experimental verification is complicated by post-selection overhead [27–29], a more fundamental challenge lies in precisely defining what constitutes a 'coding phase' in these dynamically driven systems. Our results shed light on this question for our tailored codes and the MIPT share many similarities, as discussed in SM 3.

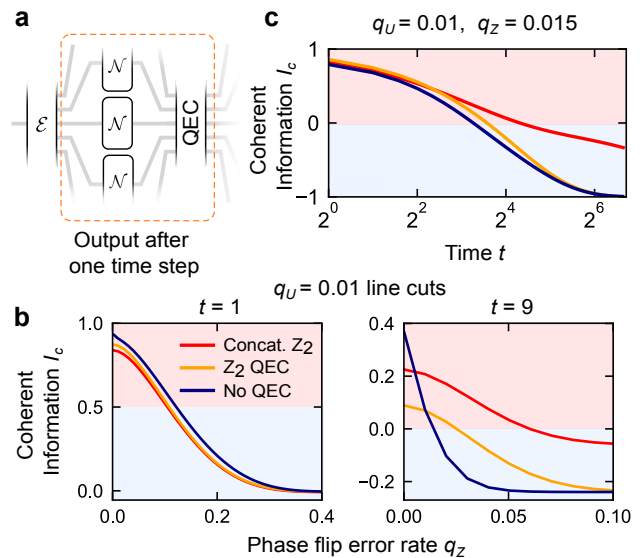


FIG. 4. **Perfect communication via many uses of a noisy channel** **a**, Output of passing a N -qubit code through m -uses of a noisy channel \mathcal{N} and a QEC layer after an encoding step \mathcal{E} . **b**, Coherent information I_c of a 3-qubit \mathbb{Z}_2 code for 3-uses of the ORUM channel i.e., $(N, m) = (3, 3)$. I_c are shown for \mathbb{Z}_2 code with no-QEC (blue), \mathbb{Z}_2 code with QEC but no repetition (orange), and the \mathbb{Z}_2 code with QEC and repetition (red) at times $t = 0$ (left) and $t = 9$ (right) for q_U line cuts along $q_U = 0.01$. Although at $t = 0$, there is no advantage from QEC, at $t = 9$, there is a clear advantage. **c**, Dynamics of the same three cases presented in **b** at $q_U = 0.01, q_z = 0.015$ showing improvement in the communication rate at long-times by leveraging the bit-flip and phase flip correction enabled by repetition.

To tailor codes for modern quantum hardware, following the optimization approach presented here, a number of challenges need to be overcome. A key step is estimating the von Neumann entropies that enter the computation of coherent information. The problem in general is challenging because the von Neumann entropy is a highly non-linear observable that is sensitive to noise. Fortunately, here it is the difference between two large entropies that is needed. Polynomial algorithms are available for this situation[30]. There are also other approximate techniques such as classical shadows[31], a combination of matrix and phase estimation[32], and quantum

neural estimation[33]. That this step is feasible is perhaps most convincingly found in a recent experimental demonstration on Quantinuum’s quantum computer[34]. Hence, there appears to be no barrier to tailoring codes to the noise profile of modern quantum computers.

II. ACKNOWLEDGEMENT

We thank Cenke Xu, Sarang Gopalakrishnan, Ehud Altman, Ashwin Vishwanath, Rahul Sahay, and Ruihua Fan for their valuable discussions during the early stages of this project.

-
- [1] D. P. DiVincenzo, P. W. Shor, and J. A. Smolin, *Phys. Rev. A* **57**, 830 (1998).
 - [2] J. J. Wallman and J. Emerson, *Physical Review A* **94**, 052325 (2016).
 - [3] A. Robertson, C. Granade, S. D. Bartlett, and S. T. Flammia, *Physical Review Applied* **8**, 064004 (2017).
 - [4] D. K. Tuckett, A. S. Darmawan, C. T. Chubb, S. Bravyi, S. D. Bartlett, and S. T. Flammia, *Physical Review X* **9**, 041031 (2019).
 - [5] R. W. Overwater, M. Babaie, and F. Sebastiano, *IEEE Transactions on Quantum Engineering* **3**, 1 (2022).
 - [6] E. T. Jaynes, *Physical review* **106**, 620 (1957).
 - [7] E. T. Jaynes, *Physical review* **108**, 171 (1957).
 - [8] J. Preskill, “Chapter 10: Quantum shannon theory,” Online Lecture Notes (2022), see <http://theory.caltech.edu/~preskill/ph219/>.
 - [9] B. Schumacher and M. A. Nielsen, *Phys. Rev. A* **54**, 2629 (1996).
 - [10] S. Lloyd, *Physical Review A* **55**, 1613–1622 (1997).
 - [11] P. W. Shor, in *lecture notes, MSRI Workshop on Quantum Computation* (2002).
 - [12] I. Devetak, *IEEE Transactions on Information Theory* **51**, 44 (2005).
 - [13] M. M. Wilde, *Quantum information theory* (Cambridge university press, 2013).
 - [14] D. Elkouss and S. Strelchuk, *Physical Review Letters* **115**, 040501 (2015).
 - [15] F. Leditzky, D. Leung, V. Siddhu, G. Smith, and J. A. Smolin, *Physical review letters* **130**, 200801 (2023).
 - [16] P. W. Shor and J. A. Smolin, “Quantum error-correcting codes need not completely reveal the error syndrome,” (1996), [arXiv:quant-ph/9604006](https://arxiv.org/abs/quant-ph/9604006) [quant-ph].
 - [17] D. P. DiVincenzo, P. W. Shor, and J. A. Smolin, *Phys. Rev. A* **57**, 830 (1998).
 - [18] F. Kianvash, M. Fanizza, and V. Giovannetti, *Quantum* **6**, 647 (2022).
 - [19] S. Roofeh and V. Karimipour, “Phase transition in the quantum capacity of quantum channels,” (2024), [arXiv:2408.05733](https://arxiv.org/abs/2408.05733) [quant-ph].
 - [20] Z. Raissi, C. Gogolin, A. Riera, and A. Acín, *Journal of Physics A: Mathematical and Theoretical* **51**, 075301 (2018).
 - [21] Y. Li, X. Chen, and M. P. A. Fisher, *Phys. Rev. B* **98**, 205136 (2018).
 - [22] Y. Li, X. Chen, and M. P. A. Fisher, *Phys. Rev. B* **100**, 134306 (2019).
 - [23] B. Skinner, J. Ruhman, and A. Nahum, *Phys. Rev. X* **9**, 031009 (2019).
 - [24] C.-M. Jian, Y.-Z. You, R. Vasseur, and A. W. W. Ludwig, *Phys. Rev. B* **101**, 104302 (2020).
 - [25] M. J. Gullans and D. A. Huse, *Phys. Rev. X* **10**, 041020 (2020).
 - [26] S. Choi, Y. Bao, X.-L. Qi, and E. Altman, *Phys. Rev. Lett.* **125**, 030505 (2020).
 - [27] C. Noel, P. Niroula, D. Zhu, A. Risinger, L. Egan, D. Biswas, M. Cetina, A. V. Gorshkov, M. J. Gullans, D. A. Huse, and C. Monroe, *Nature Physics* **18**, 760–764 (2022).
 - [28] J. M. Koh, S.-N. Sun, M. Motta, and A. J. Minnich, *Nature Physics* **19**, 1314–1319 (2023).
 - [29] J. C. Hoke, M. Ippoliti, E. Rosenberg, and D. Abanin et al., *Nature* **622**, 481–486 (2023).
 - [30] K. M. Audenaert, *Journal of Physics A: Mathematical and Theoretical* **40**, 8127 (2007).
 - [31] B. Vermersch, A. Rath, B. Sundar, C. Branciard, J. Preskill, and A. Elben, *PRX Quantum* **5**, 010352 (2024).
 - [32] A. N. Chowdhury, G. H. Low, and N. Wiebe, *arXiv preprint arXiv:2002.00055* (2020).
 - [33] Z. Goldfeld, D. Patel, S. Sreeksumar, and M. M. Wilde, *Physical Review A* **109**, 032431 (2024).
 - [34] G. Greene-Diniz, C. N. Self, M. Krompiec, L. Coopmans, M. Benedetti, D. M. Ramo, and M. Rosenkranz, *arXiv preprint arXiv:2409.15908* (2024).
 - [35] A. Paszke, S. Gross, F. Massa, A. Lerer, J. Bradbury, G. Chanan, T. Killeen, Z. Lin, N. Gimeshain, L. Antiga, A. Desmaison, A. Kopf, E. Yang, Z. DeVito, M. Raison, A. Tejani, S. Chilamkurthy, B. Steiner, L. Fang, J. Bai, and S. Chintala, in *Advances in Neural Information Processing Systems 32* (Curran Associates, Inc., 2019) pp. 8024–8035.

Supplementary Information for

Emergent coding phases and hardware-tailored quantum codes

Gaurav Gyawali, Henry Shackleton, Zhu-Xi Luo, Michael J. Lawler

1. NUMERICAL OPTIMIZATION OF THE CHANNEL CAPACITY

All the numerical calculations in this paper were done using PyTorch [35]. To compute the single-use channel capacity $Q^{(1)}(\mathcal{N})$, we define a trainable “model” using a dense representation (a Pytorch tensor) of $|\psi_{RS}\rangle$ as the initial state. Each element of the $|\psi_{RS}\rangle$ vector is a trainable parameter, much like weights in a neural network. Then we compute $I_c(|\psi_{RS}\rangle\langle\psi_{RS}|, \mathcal{N})$, where \mathcal{N} is the whole quantum channel model considered by directly implementing the superoperators corresponding to the small channels that make up \mathcal{N} via non-trainable Pytorch tensors and using `torch.einsum` to carry out the computations to produce the output density matrix $\rho_{R'S'}$. This density matrix is the largest tensor in memory, generally requiring $4n$ qubits worth of information for a n qubit system S (namely $\dim(S) = n$, $\dim(R) = n$, so its a $2^{2n} \times 2^{2n}$ matrix). Finally, we compute the von Neumann entropies $S(\rho_{R'S'})$ and $S(\rho_{S'})$ by straightforward diagonalization of the density matrices. The coherent information $I_c(|\psi_{RS}\rangle\langle\psi_{RS}|, \mathcal{N})/n$, for an n qubit system, is then the “loss function” analogous to mean squared error typically employed in training neural networks, but with the intent to maximize it rather than minimize. Finally, we update $|\psi_{RS}\rangle$ using the gradients of the coherent information and normalize $|\psi_{RS}\rangle$.

2. \mathbb{Z}_2 CODE AS A SPIN LIQUID

The \mathbb{Z}_2 code is defined as follows. Let $|\text{even}\rangle_S$ be the state

$$|\text{even}\rangle_S = \frac{1}{2^{(n-1)/2}} (|00\dots 000\rangle_S + e^{i\phi_1}|00\dots 011\rangle_S + e^{i\phi_2}|00\dots 101\rangle_S + \dots) \quad (\text{S1})$$

where the sum extends over all basis states of the system $|x\rangle_S$ with an even number of 1’s in the bit string x , each state having an arbitrary phase ϕ_i . Then define the state $|\text{odd}\rangle_S$ to be the state

$$|\text{odd}\rangle_S = \frac{1}{2^{(n-1)/2}} (|00\dots 001\rangle_S + e^{i\phi_3}|00\dots 010\rangle_S + e^{i\phi_4}|00\dots 100\rangle_S + \dots), \quad (\text{S2})$$

where the sum extends over all basis states of the system $|x\rangle_S$ with an odd number of bit strings, again each state having an arbitrary phase. Then, we can define a purification of this state observed in the quantum capacity calculations to be

$$\psi_{\mathbb{Z}_2, RS} = \frac{1}{\sqrt{2}} (|0\rangle_R \otimes |\text{even}\rangle_S + |1\rangle_R \otimes |\text{odd}\rangle_S). \quad (\text{S3})$$

and tracing over R shows us this state is

$$\rho_{\mathbb{Z}_2, S} = \frac{1}{2} (|\text{even}\rangle_S \langle\text{even}| + |\text{odd}\rangle_S \langle\text{odd}|) \quad (\text{S4})$$

The arbitrary phases that enter the purification suggest the existence of a gauge symmetry. Applying the unitary transformation $U(\{\theta_i\}) = e^{i\sum_j \theta_j n_j}$ with $n_j = (1 + Z_j)/2$ just alters the phases ϕ_1, ϕ_2 , etc. in $|\text{even}\rangle_S$. Applying a similar transformation but with $n_1 = (1 - Z_1)/2$, $n_j = (1 + Z_j)/2$, $j \geq 2$ to $|\text{odd}\rangle_S$ similarly alters its phases. But if we set $\theta_i = \pi$, then we find $|\text{even}\rangle_S \rightarrow |\text{even}\rangle_S$ and $|\text{odd}\rangle_S \rightarrow -|\text{odd}\rangle_S$ which leaves $\rho_{\mathbb{Z}_2, S}$ invariant.

To show ORUM has a gauge symmetry, let us first define it more carefully. We can write the two-qubit depolarizing channel as

$$\mathcal{U}_{i,j}(\rho) = (1 - q)\rho + q \sum_{a,b} \tau_{ia} \tau_{jb} \rho \tau_{ia} \tau_{jb} \quad (\text{S5})$$

where τ_{ia} are the identity and three Pauli operators I_i, X_i, Y_i, Z_i on site i indexed by a . We can also write the one-qubit dephasing channel as

$$\mathcal{Z}_i(\rho) = (1 - q)\rho + q Z_i \rho Z_i \quad (\text{S6})$$

Then, if we pass a gauge-transformed state $U(\{\theta_j\})\rho U^\dagger(\{\theta_j\})$ through the ORUM quantum channel, we find

$$\mathcal{Z}_i(U(\{\theta_j\})\rho U^\dagger(\{\theta_j\})) = U(\{\theta_j\})\mathcal{Z}_i(\rho)U^\dagger(\{\theta_j\}) \quad (\text{S7})$$

and

$$\mathcal{U}_{i,i+1}(U(\{\theta_j\})\rho U^\dagger(\{\theta_j\})) = U(\{\theta_j\})\mathcal{U}_{i,i+1}(\rho)U^\dagger(\{\theta_j\}) \quad (\text{S8})$$

for $U(\{\theta_j\})\tau_{ia}\tau_{i+1,b}U^\dagger(\{\theta_j\}) = \tau'_{ia}\tau'_{i+1,b}$ amounts to rotating the Pauli operators to a new local basis which still preserves the one-design property of these unitaries. Namely, after the gauge transformation, our expression for $\mathcal{U}_{i,i+1}$ has a different set of Kraus operators which define the same channel (Kraus operators are not unique). Hence, the phases we find numerically in $|\text{even}\rangle_S$ and $|\text{odd}\rangle_S$ are a consequence of a $U(1)^{\otimes n}$ gauge symmetry.

As a result of the gauge symmetry, the \mathbb{Z}_2 code is like a \mathbb{Z}_2 spin liquid, it breaks the $U(1)$ gauge symmetry of the dynamics down to the global \mathbb{Z}_2 symmetry of $\rho_{\mathbb{Z}_2,S}$.

3. MEASUREMENT-INDUCED PHASE TRANSITION

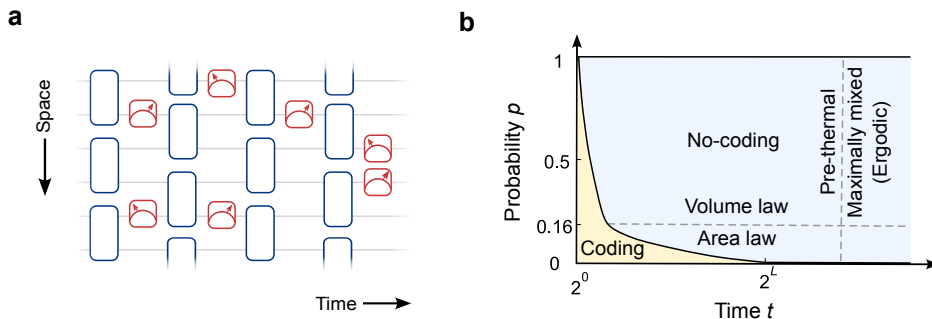


FIG. S1. **Purification in monitored circuits a**, Four layers of a monitored circuit (top), commonly used to study measurement-induced phase transition (MIPT), consisting of random 2-qubit unitaries (blue rectangles) and interspersed measurement gates (red squares) inserted with some measurement probability p . **b**, The purification phase diagram of a random Clifford model with the maximally mixed initial state. Below the critical point ($p < p_c$), the purification time diverges with the system size, whereas, for $p > p_c$, the maximally mixed state purifies at constant time.

The viewpoint of coding transition has been valuable to understanding measurement-induced phase transitions (MIPT) [25, 26]. MIPT arises due to a dynamical interplay between unitary gates vs. projective measurements, resulting in an entanglement phase transition from a volume law to an area law scaling of the entanglement entropy [21–24]. Furthermore, these transitions are also reflected in the divergence of purification time for a mixed initial state. This is a coding transition, as the purification signifies that the system no longer carries information about the initially entangled reference [25, 26]. While all states ultimately purify under monitored dynamics, they can reliably transmit quantum information for exponentially long timescales relative to system size. This phenomenon is captured in the system’s coherent information, a key measure of its capacity to carry quantum information [9]. While the coding transition provides an alternative perspective to MIPT, observing it experimentally is still challenging due to the exponential sampling complexity of post-selection [27–29]. Nevertheless, identifying coding transitions by viewing the measurement-driven circuit as a noisy quantum channel generically doesn’t require post-selection.

A typical circuit used to observe MIPT is shown in Fig. S1a (top), which consists of a “brickwork” circuit of two-qubit unitaries from, for instance, random Clifford ensemble interspersed with single-qubit measurements in the Z -basis. Starting from a pure state, the probability of measurement p , continuously drives the steady-state entanglement entropy from a volume-law to an area-law scaling [21–23]. However, one can also start from a mixed state, for instance, the maximally mixed state, resulting from an initial entanglement of the system S with a reference R . Although for any $p > 0$, the system purifies at exponentially long times, the purification time exhibits two distinct behaviors. Above a critical measurement probability p_c , the purification time is constant, whereas it sharply diverges with respect to the system size for $p > p_c$ (bottom). The p_c for the purification phase transition has been found to be the same as p_c for MIPT [25]. The purification transition is a “coding transition” because the system transitions from transmitting finite quantum information via the maximally mixed state to transmitting zero quantum information. The

coherent information $I_c = S(\rho_S) - S(\rho_{RS})$ reflects the ability of an initial state ρ_{RS} to transmit quantum information through a channel \mathcal{E} .

Our work examines the coherent information by passing various states through the channel \mathcal{E} . The maximum coherent information defines the channel capacity, see [Eq. \(2\)](#). The trajectories generated by the quantum channel, which is often expressed in an operator-sum representation with Kraus operators, are quantitatively different from those produced by the original channel. A given channel can have many Kraus representations, so the procedure for generating trajectories is not unique if we take the channel as the fundamental dynamical law. For instance, a N -qubit depolarization channel can be defined as a sum over either Pauli, Clifford or the Haar-random unitaries as long as they form a 1-design. At a trajectory level, the entanglement phase transition for the Haar-random case has a higher p_c compared to the Clifford case. However, there is no transition in the entanglement phase in the Pauli case. This seems similar to using different suboptimal codes in the approach discussed in the main text.